Comparison of mammalian cell lines expressing distinct isoforms of divalent metal transporter 1 in a tetracycline-regulated fashion

Michael D. GARRICK*†, Hung-Chieh KUO*, Farida VARGAS*, Steven SINGLETON*, Lin ZHAO*, Jaime J. SMITH*, Prasad PARADKAR‡, Jerome A. ROTH‡ and Laura M. GARRICK*§[1]

*Department of Biochemistry, SUNY, Buffalo, NY, 14214, U.S.A., †Department of Pediatrics, SUNY, Buffalo, NY, 14214, U.S.A., ‡Department of Pharmacology & Toxicology, SUNY, Buffalo, NY, 14214, U.S.A., and §Department of Medicine, SUNY, Buffalo, NY, 14214, U.S.A.

DMT1 (divalent metal transporter; also known as SLC11A2, DCT1 or Nramp2) is responsible for ferrous iron uptake in the duodenum, iron exit from endosomes during the transferrin cycle and some transferrin-independent iron uptake in many cells. Four protein isoforms differ by starting in exon 1A or 2 and ending with alternative peptides encoded by mRNA that contains or lacks an IRE (iron responsive element; ±IRE). We have compared 1A/+IRE and 2/−IRE DMT1 during regulated ectopic expression. HEK-293-F (human embryonic kidney-293-fast growing variant) cells were stably transfected with each construct expressed from a tetracycline-regulated CMV promoter. Reverse transcriptase-PCR analysis showed that construct expression responded to doxycycline. Immunofluorescence staining of cells, using antibodies specific for DMT1 isoforms, confirmed an increase in expression in the plasma membrane and cytosolic vesicles after doxycycline treatment, but with isoform specific distributions. Immunoblotting also revealed stimulation of expression.

Nevertheless, both DMT1 isoforms performed similarly in assays for functional properties based on $^{54}Mn^{2+}$ and $^{59}Fe^{2+}$ uptake. Mn incorporation after doxycycline treatment was $\sim$10-fold greater than that of untreated cells, while expression in the untreated cells was $\sim$5-fold greater than in the untransfected cells. Uptake of Mn depended on addition of doxycycline, with half maximal response at $\sim$1 nM doxycycline. Doxycycline-stimulated Mn and Fe uptake was linear with time for 10 min but not over longer periods. Transport exhibited a pH optimum at $\sim$5.5 and dependence on incubation temperature and Mn or Fe concentration. The new cell lines should prove useful for research on metal homoeostasis, toxicological studies and efforts to identify distinctive properties of the isoforms.

Key words: DMT1, iron, iron response element (IRE), Manganese, metal transport, tetracycline induction.

INTRODUCTION

Iron and manganese are required nutrients, but both are potentially toxic (reviewed in [1,2]), therefore they must be carefully managed. DMT1 [divalent metal transporter1; also known as SLC11A2 (solute carrier 11 group A member 2), DCT1 (divalent cation transporter 1) or Nramp2 (natural resistance associated macrophage protein 2)] is the major duodenal transporter for absorption of ferrous iron [3–5], but it also participates in ferric iron transport by aiding ferrous iron exit from endosomes during the transferrin cycle [5,6]. One mode of NTBI (non-transferrin bound iron) uptake relies on DMT1 [7,8]. It is therefore worthwhile to examine how DMT1 function affects the levels of iron and manganese in cells. As DMT1 may also transport six or more other divalent metal ions [3], its function could also be relevant to the nutrition of copper, cobalt and zinc, and to their toxicity and that of nickel, cadmium and lead. Whether all these metals are actually transported by DMT1 has not been resolved [9,10]. We therefore developed cell lines that selectively express DMT1, to investigate these issues and to gain insight into the occurrence of DMT1 isoforms.

DMT1 has at least four isoforms: two are derived from N-terminal alternatives and two are from C-terminal alternatives. Alternative promoters, presumably, allow transcription to start at exon 1A or exon 1B [11]; exon 1B is not translated, so mRNA

that is transcribed from exon 1B will encode a protein whose translation starts in exon 2. Rat exon 1A mRNA leads to an N-terminal extension of 31 amino acids. At the 3′ end, alternative poly-adenylation generates mRNA species that contain or lack an IRE (iron responsive element; herein referred to as ±IRE). The 3′ IRE could affect mRNA stability, however Wardrop and Richardson [12] questioned this assumption. Although the central exons 2–16 encode 543 amino acids in common, their C-terminals differ by 18 (+IRE) or 25 (−IRE) residues. The alternative isoforms of DMT1 are 1A/+IRE, 1A/−IRE, 2/+IRE and 2/−IRE (where 1A and 2 refer to the exon that carries the translation start site and ±IRE refers to the presence or absence of the IRE). We cloned and expressed 1A/+IRE and 2/−IRE to see how differences at either end of DMT1 affected its properties.

DMT1 has a role in gastrointestinal uptake of metals and in transferrin dependent trafficking of iron and, to an extent, manganese (for recent reviews see [2,13]). DMT1s role in the homoeostasis of other metals and in metal toxicity requires further characterization. NTBI absorption may cause pathological internal exposure of cells to iron or manganese, but such uptake may also be a protective response [14–20]. DMT1 may also transport other metals that are toxic such as nickel, cadmium and lead [21–25]. In the present report, the cell lines provide the opportunity to examine whether metal uptake is protective and helps to minimize pathology or, alternatively, if it is toxic. Here

we show that the two isoforms (1A/+IRE and 2/−IRE) are, as expected, expressed in different subcellular locations, however they unexpectedly share all the assessed functional properties, despite their distinct localizations.

EXPERIMENTAL

Materials

PerkinElmer supplied $^{59}FeCl_3$ and $^{54}MnCl_2$. All other reagents were from Sigma except where indicated.

DNA constructs

Cloning of rat 1A/+IRE and mouse 2/−IRE DMT1 cDNA into the Gateway® system has been described previously [26]. Constructs were made containing the cDNA or the cDNA plus an N- or C-terminal FLAG-tag. Using this system, the constructs were subcloned into pDEST31.

Cell lines and cell culture

HEK-293-F (human embryonic kidney 293-fast growing variant) cells contained a TetR:Hyg element for β testing (Invitrogen). These tetres (tetracycline responsive) cells were maintained at $37\,°C$ with 5 % CO_2 in Dulbecco's modified Eagle's medium with non-essential amino acids and 10 % (v/v) FBS (foetal bovine serum; Clontech) containing $200\,\mu g/ml$ of hygromycin, $100\,\mu g/ml$ of streptomycin and 100 units/ml of penicillin (all from Invitrogen). Using Geneticin (G418 at $600\,\mu g/ml$; Invitrogen) selection, we obtained stably transfected cell lines that contained the empty pDEST31 vector or the same vector containing one of the following constructs: mouse FLAG-tagged (C-terminal) 2/−IRE-DMT1; rat FLAG-tagged (N-terminal) 1A/+IRE-DMT1; or rat 1A/+IRE-DMT1. The CMV promoter of pDEST31 is adjacent to a tet-on site. To maintain these cell lines, one must avoid using FBS that contains tetracycline, therefore we always used certified FBS (Clontech). The cell lines were used in experiments after 10–30 passages. Cells containing DMT1 constructs were grown with doxycycline or untreated, however those containing only the tetres element or the tetres element plus the empty vector were indistinguishable whether they were exposed to doxycycline or untreated prior to any experiment. Except where indicated, exposure to doxycycline (50 nM) was for 24 h.

The parental tetres cell line contained a DNA construct that encoded a modified tet-repressor that allowed a tet-on response; this line was maintained by hygromycin selection. Tetres cells transfected with the empty pDEST31 vector, or constructs derived from it, were selected for Geneticin resistance and cloned. Individual clones were screened initially by immunofluorescence microscopy, which allowed the detection of increased expression in the presence of doxycycline. The screen used antibodies specific for the +IRE epitope, the −IRE epitope and/or the FLAG epitope. We selected, for further characterization, the clones that appeared to give the greatest increase in expression when doxycycline was added.

RT (reverse transcription)-PCR

Total RNA from the cell lines was collected using TRIzol® (Invitrogen) reagent following the manufacturer's protocol. RNA was quantified by spectrophotometry and 500 ng of RNA was used in each reaction. RT-PCR was performed using the Superscript (Invitrogen) one-step RT-PCR system for 25, 30 or 35 cycles in an Eppendorf Mastercycler. The two different extents of amplification allowed better estimation of the relative degrees of expression. The primers used for rat DMT1 mRNAs were as follows:

5′-GCTGAGCGAAGATACCAGCG-3′ (forward), 5′-TGTGC-AACGGCACATACTTG-3′ (reverse) for +IRE; 5′-AAGGCGA-AGAAGATCTGGAG-3′ (forward), 5′-CCACAGGCCGCTGT-TTG-3′ (reverse) for −IRE; and 5′-TCCGATGGGGAAGAAGC-AGCC-3′ (forward), 5′-GGATCTGTGCTCTTAGAATAGG-3′ (reverse) for 1A. The primer set for mouse −IRE DMT1 was 5′-CGCCCAGATTTTACACAGTG-3′ (forward) and 5′-AAGC-TTCACTACCTGCACAC-3′ (reverse) with a product size of 351 bp. The primers for β-actin were 5′-CACCACAGCTGAG-AGGGAAATCGTGCGTGA-3′ (forward) and 5′-ATTTGCGGT-GCACGATGGAGGGGCCGGACT-3′ (reverse). The PCR products were electrophoresed in 2 % (w/v) agarose gel containing ethidium bromide and imaged under UV light.

Immunofluorescence microscopy and immunoblotting

Immuno-affinity purified polyclonal rabbit antibodies specific for the +IRE and −IRE isoforms of rat DMT1 were characterized earlier [27], while the antibody for the 1A form was described more recently [26]; murine monoclonal antibody directed against the FLAG-epitope tag was from Sigma. Slides were prepared and examined by confocal microscopy as described previously [26]. Cells were lysed, the lysates resolved by SDS/PAGE (4–15 % gradient gels), and blotted and immunostained also as described previously [26].

Incubations with radiolabelled metal ions

Cells were grown to ~60 % confluence in 6-well plates with doxycycline or without, as described above. Doxycycline was added to selected wells and cultures were grown for 24 h except where indicated. Cells were gently washed twice in prewarmed wash buffer [10 mM Hepes (pH 7.4), 150 mM NaCl, 1 mM $CaCl_2$ and 1 % (w/v) glucose]. Hepes was supplemented with 10 mM Mes when pH optima were determined. Incubations were at $37\,°C$ in Hepes buffer at pH 6.0 except where indicated. We generated $^{59}Fe^{2+}$ from $^{59}FeCl_3$ by adding a 10-fold excess of unlabelled $FeSO_4$ and a 100-fold excess of ascorbic acid [8,28]. Iron was then added to incubations to initiate the uptake as Fe^{2+}. The concentration of $^{59}Fe^{2+}$ was 100 nM except where indicated. Manganese was added directly as $^{54}MnCl_2$ and incubated for 10 min. Except where indicated the concentration of $^{54}Mn^{2+}$ used was 10 nM. Incubations were terminated by removing the uptake buffer and gently replacing it with a stop buffer (wash buffer with 10 mM NaF and 20 mM 2-deoxy-D-glucose, pH 7.4) at $4\,°C$. Cells were then collected into microcentrifuge tubes with a cell scraper and recovered by centrifugation. $^{54}Mn^{2+}$ incubations were washed twice with stop buffer containing unlabelled 1 mM $MnCl_2$, while $^{59}Fe^{2+}$ incubations were washed with stop buffer containing 1 mM desferrioxamine. Cells were resuspended in 1 ml of wash buffer and counted in an LKB Compugamma 1282 γ counter.

In control experiments (results not shown), we compared the stop buffer with buffers lacking unlabelled $MnCl_2$ or desferrioxamine, or with stop buffer containing 1 mg/ml pronase to eliminate surface bound radioactivity. The selected stop buffer was optimal, so designating the apparent incorporation as uptake is justified, although a minute portion could still be due to surface labelling.

Statistical considerations

The number of replicates for each experiment varied, but it was always at least two, and it has been indicated where more were used. Where appropriate, data were analysed by multiple regression or ANOVA using Stata (StataCorp). For nonlinear least squares analyses to fit Michaelis–Menten curves, Scientis (MicroMath) was applied; then for comparisons, two-tailed t tests were performed as described previously [6], except that parameters
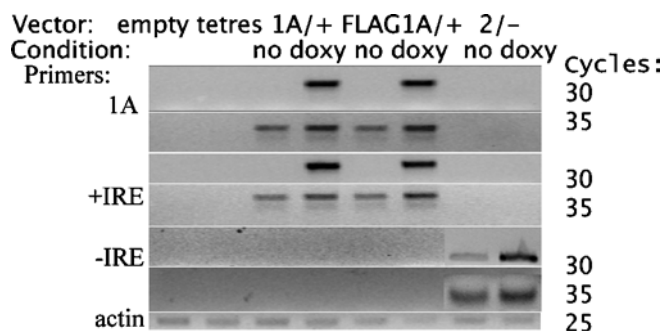
Figure 1   RT-PCR analysis of DMT1 mRNA expression for the cell lines

The vector is indicated above the images and with doxycycline (doxy) or without (no) for the three inducible cell lines. The choice of the primer pair for amplification is shown on the left-hand side. On the right-hand side, the number of cycles allows an estimate of the relative extent of expression for the mRNA constructs. Results for the top four rows (1A and +IRE primers, cycles 30 and 35) were obtained using rat-specific primers for all eight conditions as indicated. The results for the mouse 2/−IRE DMT1 primers are placed over the results for rat 2/−IRE DMT1 primers in the last two columns (2/− no and 2/− doxy) of the two rows corresponding to the −IRE primers for 30 and 35 cycles. Actin was used as a loading control.

were reported by Scientis not MINSQ. Significance required $P \leqslant 0.05$.

RESULTS

Doxycycline regulated expression of DMT1 mRNA isoforms

Analysis by RT-PCR (Figure 1) shows that DMT1 mRNA expression increased considerably for each of the cell lines when doxycycline was present in the culture medium. Expression of the mRNA was still detectable when the cells were grown without doxycycline, but much less compared with the fully induced cells. Using the number of PCR cycles as a guide, we estimate that the 1A/+IRE and FLAG–1A/+IRE constructs have $\sim$12-fold (range 8–32-fold) more mRNA when induced compared with uninduced cells, while the 2/−IRE construct has $\sim$10-fold (range 6–24-fold) more mRNA. Expression is undetectable when the cell line contains no DMT1 construct (tetres and empty), or when the primers are not designed for the construct present in the particular cell line (for example, 1A and +IRE primers on mRNA from 2/−IRE cells, or −IRE primers on mRNA from either 1A/+IRE or FLAG–1A/+IRE cells). Although the HEK-293-F cells should also express human DMT1 isoforms endogenously, the primers are species specific, therefore endogenous expression is not detected.

Doxycycline regulated expression of DMT1 protein isoforms

The FLAG-tag allows verification that this epitope co-localized in confocal sections with the particular epitopes present in the transporter (see supplementary Figure S-1 at http://www.BiochemJ. org/bj/398/bj3980539add.htm). Much lower expression was detected for 2/−IRE-DMT1 without doxycycline (Figure S-1, panels A–C) compared with high level expression induced by doxycycline (Figure S-1, panels D–F). Similarly the +IRE and FLAG-epitope tag of the FLAG–1A/+IRE line exhibited increased expression after induction with doxycycline (Figure S-1, panels J–L) compared with the uninduced cells (Figure S-1, panels G–I). The titre of the antibodies and settings for the confocal microscope had been selected for placing the extents of expression at extremes, however when they were adjusted so that uninduced expression led to much brighter images (results not shown), the empty and tetres controls exhibited almost undetectable

expression of endogenous DMT1 epitopes and, as expected, undetectable expression of the FLAG-epitope tag. The cellular localization of expressed epitopes in the uninduced 2/− IRE and 1A/+IRE cell lines (results not shown) remained, under these conditions, the same as the induced expression, as shown in Figure S-1.

Although all three lines (the 2/− IRE in Figure S-1, panels D–F; the FLAG–1A/+IRE shown in Figure S-1, panels J–L; and the 1A/+IRE shown in Figure S-1, panel N) exhibited strong induction in the presence of doxycycline, the two distinct isoforms of DMT1 exhibited different localization. The 2/− IRE species has a punctate appearance and is primarily in the cytosol, while the 1A/+IRE form localizes predominantly on or near the plasma membrane. This difference is not due to the FLAG-epitope tag, which was fused onto two of the DMT1 species, as the 1A/+IRE DMT1 that lacks the FLAG-epitope tag (Figure S-1, panel N) has a similar localization as the FLAG–1A/+IRE DMT1.

Immunoblotting also detected increased expression (see supplementary Figure S-2 at http://www.BiochemJ.org/bj/398/ bj3980539add.htm). Although multiple bands apparently stain lightly for FLAG in the absence of doxycycline (Figure S-2 panels A and B), doxycycline exposure increased staining primarily at $\sim$90 kDa and to a lesser degree at $\sim$125 kDa (Figure S-2, panel A), while similar increases resulted in a smear at higher molecular mass (Figure S-2, panel B). These results show clearly that doxycycline increased the expression of the DMT1 constructs. Staining with antibody against the region coded for by exon 1A on Western blots from 1A/+IRE cells treated with doxycycline, or untreated, and on the empty vector cell-line [29], also revealed an increase in expression after doxycycline treatment, however the analysis was complicated by several apparently endogenous bands for DMT1. Antibody against +IRE DMT1 also detects increased expression of the 1A/+IRE DMT1 constructs with doxycycline (results not shown), consistent with the above data from the RT-PCR analysis and immunofluorescence studies.

Doxycycline regulated expression of DMT1 transport activity

The incorporation assay allowed evaluation of the response of $^{54}Mn^{2+}$ uptake to doxycycline concentration (Figure 2). The effective concentration of doxycycline was in the low nmol range for both 2/− IRE DMT1 and 1A/+IRE DMT1 (Figures 2A and 2B), which is the range expected for this system [30]. Maximal response occurred by 24 h and continued at least to 72 h, while the initial rise was linear with time during the first 24 h (Figure 2C).

Figure 3 shows that doxycycline induced expression was $\sim$10-fold greater than uninduced expression, however uninduced expression was also $\sim$5-fold higher than endogenous levels. Presumably mRNA expression is leaky because the CMV (cytomegalovirus) promoter is not fully repressed when doxycycline is absent. Overall elevation of DMT1 expression is $\sim$50-fold compared with cells transfected with the empty vector and untransfected cells. Endogenous $^{4}Mn^{2+}$ uptake is not necessarily due only to DMT1, so the elevation of DMT1 could be > 50-fold. This level of induction of the two isoforms of DMT1 permitted detailed comparison of the properties of the isoforms. As they are expressed in different subcellular locales, the comparison tests the hypothesis that properties of the transporter differ when it is expressed in different parts of the cell.

DMT1 transport activity is time dependent

Induced expression characterizes DMT1 rather than other possible transporters, because $\geqslant 98\%$ of uptake represents DMT1. Figure 4 presents the time course of divalent metal ion uptake
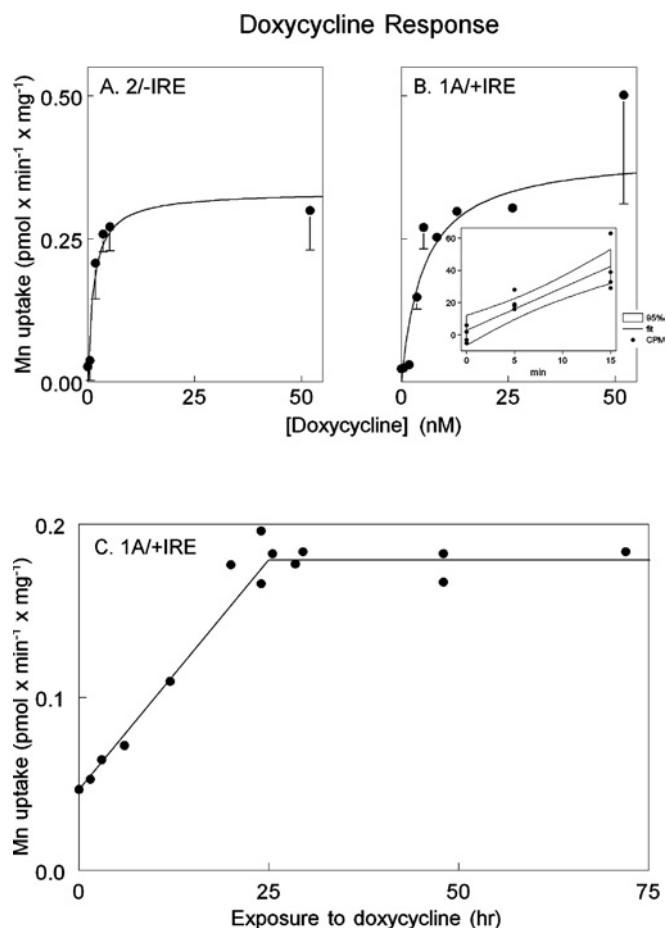
Doxycycline Response

Figure 2   Response of Mn transport to doxycyline

The 2/−IRE cell line (**A**) or the 1A/+IRE cell line (**B**) were grown to ∼60% confluence and then exposed to the concentrations of doxycyline indicated for 24 h. We calculated the rate of uptake of Mn without doxycyline treatment, as illustrated for the 1A/+IRE cells in the inset panel. Multiple wells are represented by a single point showing incorporated $^{54}Mn^{2+}$ at the indicated time. The counts/min incorporation data were fitted to a linear regression and the 95% confidence interval calculated. Each point in the larger plots was the slope of a regression expressed as pmol/min per mg of cell protein and error bars indicate the confidence interval. (**C**) The 1A/+IRE cell line was exposed to 50 nM doxycyline for the times indicated and $^{54}Mn^{2+}$ incorporation was determined over a 10 min period. We obtained similar data for the 2/−IRE cell line after 24, 48 and 72 h of doxycyline exposure, but did not examine the first 24 h as extensively (results not shown).

in the cell lines. Uptake appears greater for Fe^{2+} than for Mn^{2+}, but the apparent difference actually represents the need to use a higher concentration of the former, because the $^{59}Fe^{3+}$ had to be converted into Fe^{2+}. Incorporation of both metal ions was linear for less than 15 min when the cells were induced by doxycyline. By this time 30% of the manganese and 15% of the iron had been taken up by the cells. Incorporation in the absence of doxycyline is linear for the time period shown, however only approx. one-tenth as much manganese or iron was transported.

DMT1 transport activity is dependent on metal ion concentration

Figure 5 shows the concentration dependence of Mn and Fe transport in the cell lines. All eight curves fitted a single process well; Lineweaver–Burk plots (Figure 5, inset panels) indicate that there are no systematic deviations from Michaelis–Menten kinetics. Table 1 contains the calculated K_m and V_{max} for each curve. The data indicate that doxycycline induced transport is 11- to 15-fold greater than uninduced transport and that both isoforms
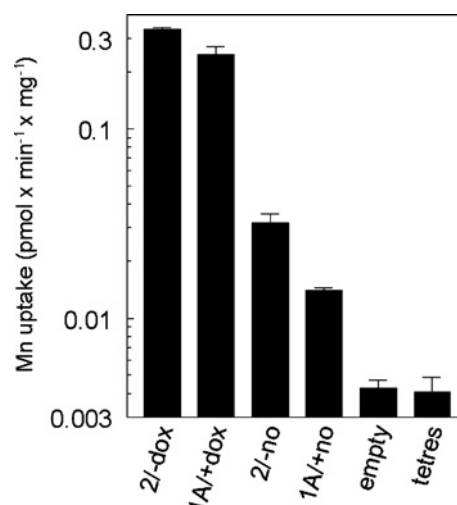

Figure 3   Increase in Mn transport due to induction of DMT1 expression

$^{54}Mn^{2+}$ uptake was compared in the inducible cell lines with doxycycline (2/−dox and 1A/+dox) or without (2/−no and 1A/+no) and in the cell lines containing the empty vector or the tetres element only. Uptake is plotted logarithmically to allow the range of response to be shown. This comparison is representative of four repetitions. Although doxycycline might increase or decrease incorporation in cell lines containing empty vector or the tetres element only, transport was unaffected (0.10 < P < 0.95 for six independent comparisons).

of DMT1 have a slightly higher affinity for Mn^{2+} compared with Fe^{2+}.

Because the Scientis software reports a standard deviation for the V_{max} and K_m, we could test the significant differences by a t test. We have reported here only selected comparisons that could have biological relevance and we have not corrected for multiple tests, because it is unclear how to do so when one is testing nonlinear fits. The most relevant K_m comparisons are the values for Mn to Fe. Two such comparisons were significant: 2/−IRE induced by doxycycline ($P = 0.001$) and uninduced ($P = 0.01$); but, although 1A/+IRE cells also exhibited a trend for the Fe K_m to be larger, it did not reach significance when comparing tetracycline induction ($P = 0.06$) with uninduced cells ($P = 0.11$). V_{max} comparisons for the effect of doxycycline were all highly significant on 2/−IRE expression with Mn ($P = 0.0001$), 2/−IRE expression with Fe ($P = 0.0001$), 1A/+IRE expression with Mn ($P = 0.002$) and 1A/+IRE expression with Fe ($P = 0.003$). It is noteworthy, however, that the K_m for Mn^{2+} for the 2/−IRE DMT1 did not differ significantly from that for 1A/+IRE DMT1, nor were the K_m values for Fe^{2+} significantly different for the two DMT1 isoforms.

Data (results not shown) for concentration dependence with tetres or empty vector containing cells exhibit more scatter and a poorer fit to a single process, probably due to lower rates of incorporation and contributions by multiple endogenous transporters. Differences between uninduced and induced cells could also come, in part, from multiple transporters, a hypothesis that predicts that the K_m values would be different for such a comparison. When the substrate was Mn, differences were not significant; however, differences were significant when Fe was substrate, with $P = 0.02$ for the 2/−IRE cells and $P = 0.04$ for the 1A/+IRE cells.

DMT1 transport activity is pH dependent

Hypothetically, DMT1 is a proton symporter requiring a proton gradient as a source of energy for metal ion transport. Supplementary Figure S-3 (see supplementary data at http://www.
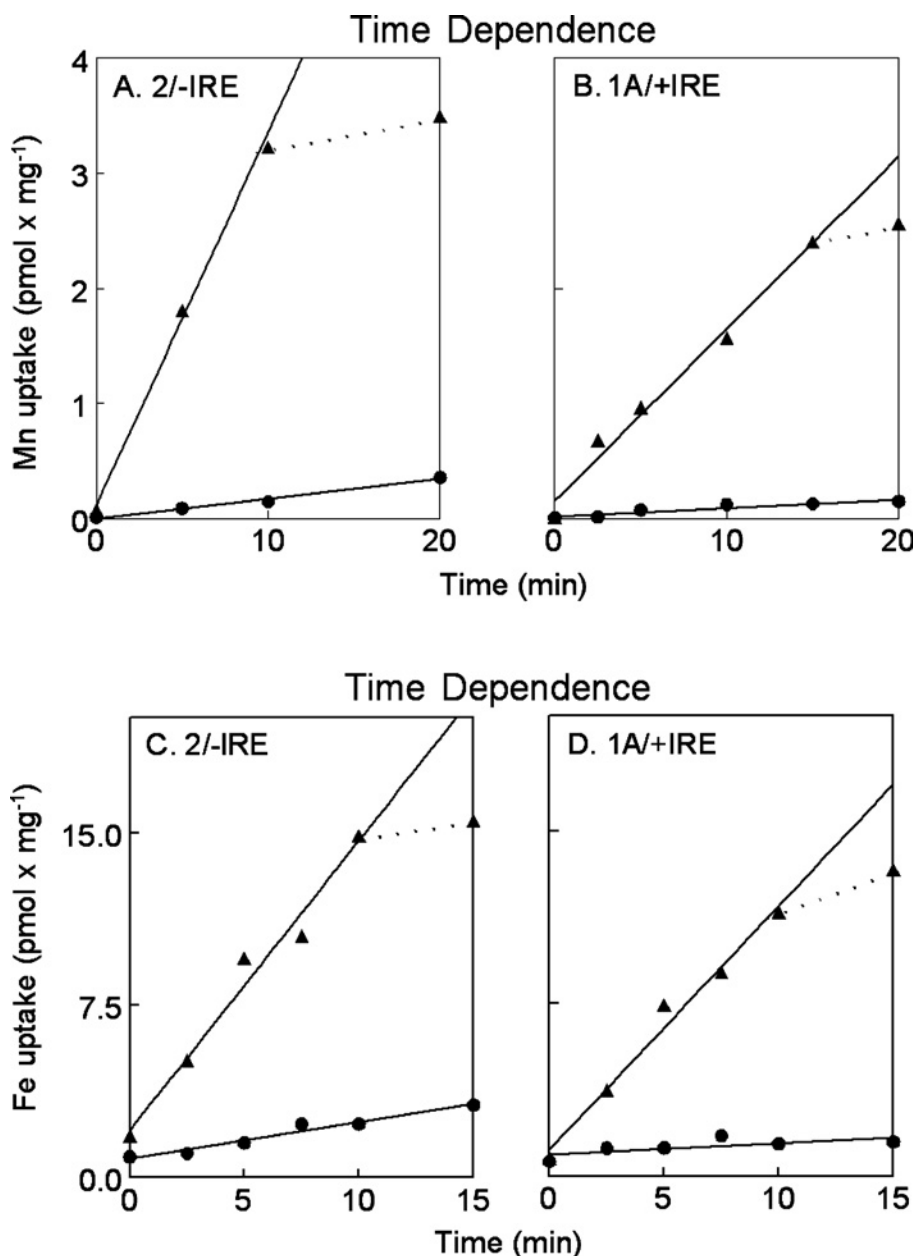
Time Dependence

Time Dependence

Figure 4   Time dependence of divalent metal ion transport

[54]Mn^{2+} (**A** and **B**) and [59]Fe^{2+} (**C** and **D**) uptakes were compared in the 2/− IRE cell line (**A** and **C**) or the 1A/+ IRE (**B** and **D**) cell line in each case with doxycycline (▲) or without (●). Lines (—) were fitted by regression for the entire time course in the latter situation, but for the first 10 min in the former with the actual extension (· ·) also shown. Time dependence was examined in six experiments for Mn and five for Fe.

BiochemJ.org/bj/398/bj3980539add.htm) shows the pH dependence of Mn and Fe uptake by the cell lines. We experienced some difficulty in getting reliable data for cells at pH values of 5.0 and 4.5 due to toxicity, which is noted in the Figure legend, however the transporter had an optimum pH of 5.5. We selected a pH of 6.0 for most studies to avoid any concern that damage to the cells affected the data.

Doxycyline stimulated metal ion uptake at each pH, the most notable being a 3- to 7-fold stimulation at pH 7.4. This observation suggests that transport can occur in the absence of a proton gradient. Without doxycycline treatment, the pH response exhibits two optima, one is at pH 7.4 and the other is more acidic. The metal ion uptake at a more acidic pH probably represents primarily DMT1 activity; while the transport at pH 7.4 could represent an

alternative uptake pathway. The data for pH dependence with tetres or empty vector containing cells (results not shown) are also bimodal probably due again to lower rates of incorporation and contributions by multiple endogenous transporters.

DMT1 transport activity is temperature dependent

Many biological processes have a Q_{10} of ~ 2, but phase transitions usually affect those occurring in membranes when the temperature is $< 12 \, ^{\circ}$C. The response of Mn and Fe uptake by the cell lines to temperature exhibits these properties (see supplementary Figure S-4 at http://www.BiochemJ.org/bj/398/bj3980539add.htm). Above 12 $^{\circ}$C, the rate of transport approximately doubles with a 10 $^{\circ}$C rise in temperature; but uptake is essentially abolished at
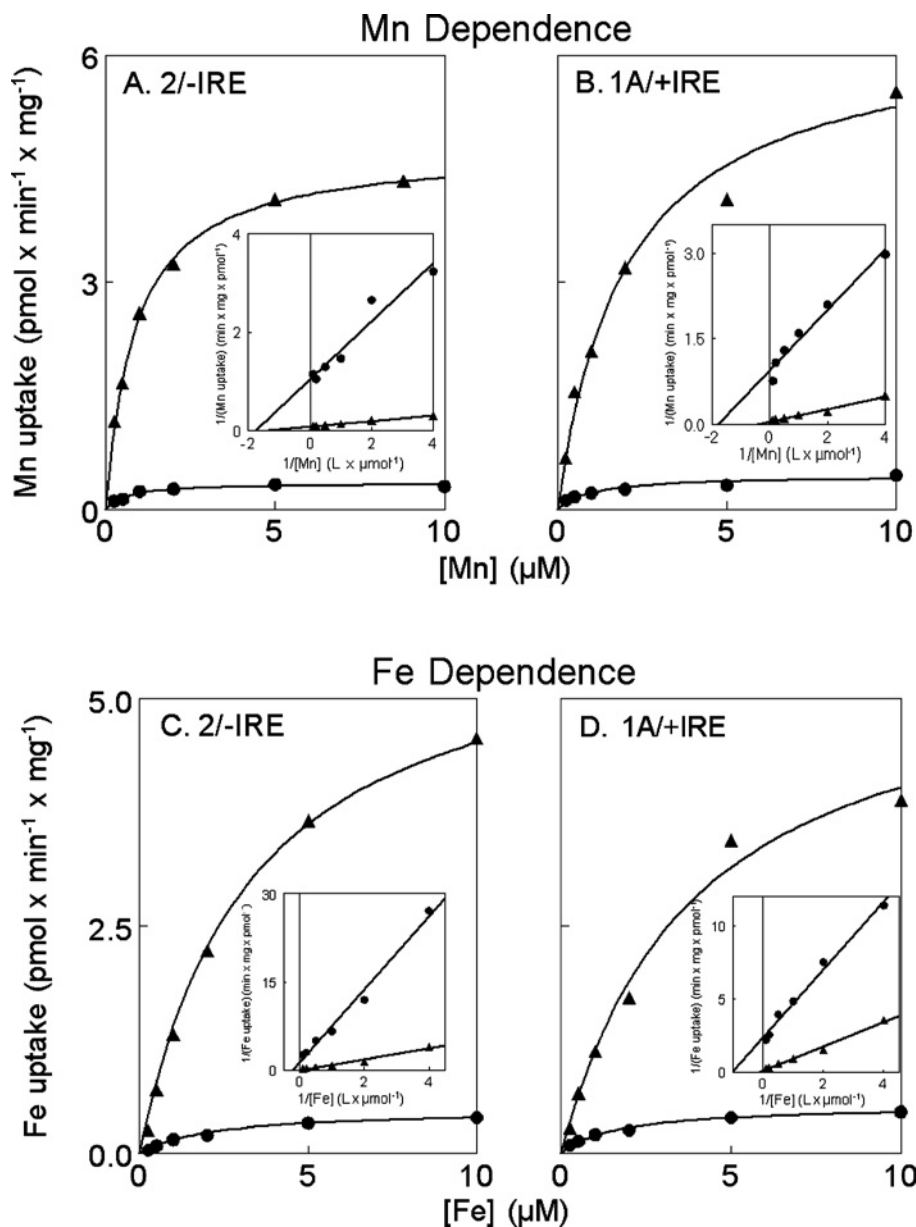
Mn Dependence

Fe Dependence

Figure 5   Concentration dependence of divalent metal ion transport

[54]Mn^{2+} (**A** and **B**) and [59]Fe^{2+} (**C** and **D**) uptake were compared for the 2/− IRE line (**A** and **C**) or the 1A/+ IRE line (**B** and **D**) in each case with doxycycline (▲) or without (●). Lines were fitted by nonlinear regression to Michaelis–Menten kinetics using the Scientis program. The inset panels show the same data linearized by the Lineweaver–Burk conversion.

the lowest temperature. Possibly the miniscule amount of apparent transport at 0 °C represents surface binding of Mn or Fe by DMT1 on the plasma membrane.

Competition between metals for DMT1

Figure 6 shows Fe^{2+} competition with Mn^{2+} as substrate, indicating classical competitive inhibition. The IC$_{50}$, estimated graphically, is ∼ 2.1 μM for Fe^{2+}, which is comparable with the K_{m} value shown in Table 1. Mn uptake was greater with 0.01 and 0.1 μM Fe^{2+} than when iron was absent, indicating that very low levels of Fe appear to stimulate Mn transport, a phenomenon also observed when Ni competed for DMT1 with Fe [21]. This approach permits us to examine competition between metal ions; the results for a series of such ions have been published elsewhere [9].

DISCUSSION

In the present report, we show that the two cell lines we constructed with isoforms of DMT1, namely mouse 2/− IRE and rat 1A/+ IRE, transcribed each construct under the control of a doxycycline inducible promoter. When cells were not treated with doxycycline, the CMV promoter was not fully repressed, therefore substantial expression still occurs. The cell lines express the two DMT1 species in different intracellular locations, with the 2/− IRE form more intracellular, in a primarily perinuclear distribution and the 1A/+ IRE form was distributed on or just below the plasma membrane. Others have observed similar distinctions in localization [27,29,31,32]; recently the structural determinants for the internalization of the − IRE forms have been, as expected, narrowed to the C-terminal of the protein [33]. Despite the difference in intracellular distribution, the two lines elevated

Table 1 Parameters for fitting concentration curves

Calculated from Figure 5 using a nonlinear least squares fit to a K_m curve using the Scientis program.

Cell line	Condition	Metal ion	K_m (μM)	Limits*	V_{max}[†]	Limits*
2/−IRE	Doxycycline	Mn^{2+}	0.87	0.68–1.06	4.8	4.4–5.1
2/−IRE	None	Mn^{2+}	0.60	0.08–1.10	0.34	0.26–0.42
1A/+IRE	Doxycycline	Mn^{2+}	2.0	0.23–3.8	6.4	4.4–8.3
1A/+IRE	None	Mn^{2+}	1.0	−0.4–2.4	0.44	0.26–0.62
2/−IRE	Doxycycline	Fe^{2+}	3.3	2.8–3.8	6.1	5.6–6.5
2/−IRE	None	Fe^{2+}	2.2	1.1–3.2	0.48	0.39–0.56
1A/+IRE	Doxycycline	Fe^{2+}	3.9	0.8–7.0	5.6	3.7–7.5
1A/+IRE	None	Fe^{2+}	1.6	0.6–2.6	0.52	0.41–0.63

* 95 % confidence limits.
[†] Measured in pmol/min per mg of protein.
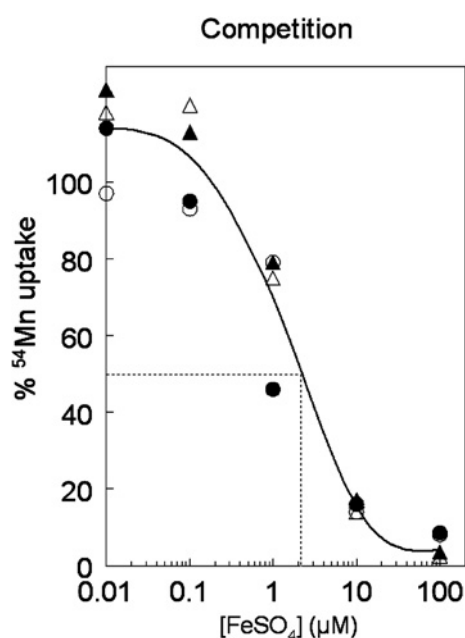
Figure 6 Competition between Fe^{2+} and Mn^{2+} for DMT1 transport

Cells were incubated with $^{54}Mn^{2+}$ and selected concentrations of FeSO$_4$ with doxycycline (▲ and △) or without (● and ○) for the 2/−IRE (▲ and ●) and the 1A/+IRE (△ and ○) cell lines. Although induced incorporation in the presence of doxycycline was 10- to 15-fold greater than without induction, the incubation without FeSO$_4$ was treated as 100 % uptake for each series to allow comparisons. We fit the concentration response with a single cubic spline because the four series of competitions were indistinguishable. Dropping a line from the 50 % level yielded an IC$_{50}$ at 2.1 μM.

the levels of DMT1 protein in response to induction. More remarkably, they exhibited very similar activities in the transport assay for both Mn^{2+} and Fe^{2+}, including the extent to which transport was induced by doxycycline. These results indicate that the two distinct isoforms can function similarly in NTBI uptake and in Mn^{2+} transport despite their different distributions in the HEK-293-F cells.

This similarity in the transport assay is relevant to earlier studies defining the functions of DMT1. As mentioned in the Introduction, DMT1 is clearly responsible for most duodenal uptake of ferrous iron [3–5] in a process similar to NTBI uptake. A G185R mutation in DMT1 also depresses release of iron from endosomes during the transferrin cycle [5,6], a possibility anticipated by Bowen and Morgan [34]. Evidence to date suggests

that the 1A/+IRE isoform is the apical transporter in enterocytes [11,29,35], while there are suggestions that the 2/−IRE form might be involved in the endosome [31–33,36]. In some specific cells, a DMT1−IRE related immunofluorescence signal was even detected in the nucleus [27], but such a distribution does not occur in HEK-293 cells with any known DMT1 isoform [26], so only the plasma membrane and endosomal localizations are relevant to the current analysis. If functional specialization normally occurs *in vivo*, why is it not evident in the cell lines, particularly if the two DMT1 species localize differently, as seen in Figure S-1? Perhaps, both isoforms are able to access each other's locations readily when highly expressed even though their equilibrium distribution is distinct. The end result is similar transport activities (qualitatively and quantitatively). There are clear indications that the apical form of DMT1 in enterocytes and Caco-2 cells, a model for the enterocyte, moves into the cytosol after exposure to iron [37,38] and this form is probably the 1A/+IRE species. It is also possible that one isoform normally acts as a surface-bound transporter to internalize metal ions, while the other species behaves more like a receptor in an endocytic process so that the different DMT1 species cooperate in its overall functions.

Induced expression of DMT1 is so high that a significant portion of the trace amounts of Mn and Fe has entered the cell within 10–15 min. As a result, the assay for uptake becomes nonlinear (Figure 4). The nonlinearity could occur because of a specific export process such as is attributed to MTP1/IREG1/Ferroportin [39–41] or it may be the result of mass action with enough Mn or Fe internalized to reverse the uptake process. The ability to increase internal Fe in a regulated fashion also suggests that the cell lines could prove useful in characterizing expression of MTP1.

DMT1 has an acidic pH optimum at ∼5.5. This response clearly adapts the transporter to the environment in the proximal duodenum and the endosome. It is also the basis of the inference that a proton gradient is the motive force for metal ion transport by DMT1. It has been postulated [42,43] that there is slippage, such that the stoichiometry of metal ion and proton may be one when there is a moderate gradient of protons, but considerably less than one when the proton gradient is stronger. The evidence supports the argument well, but if the subsurface pH for cells is 7.2 and a proton gradient is the only driving force, then there should not be any metal ion transport when the external pH is 7.4. Figure S-3, however, shows that substantial transport occurs at pH 7.4. Others have reported similar observations [44,45]. It is possible that metal ion uptake at pH 7.4 depends on bulk uptake of the fluid phase as an initial step, and then on vesicle acidification and DMT1 transport for a later step. This interpretation requires that the fluid phase uptake is not rate limiting. The lack of an initial proton requirement also provides evidence that DMT1 accounts for some NTBI uptake in tissues and cells that are not intestinal. Mackenzie et al. have also detected DMT1 metal ion transport activity when the external pH is 7.5 [46] and reached the same conclusion.

The cell lines presented in the current work have allowed thorough characterization of DMT1 isoforms, while seeking, and not finding, a functional difference. This characterization raises new and interesting questions about the properties of this transporter and on functional differences among its isoforms. We expect that the cell lines should help us and others in additional studies including: (a) how DMT1 participates in acquisition and trafficking of other metal ions; (b) whether DMT1 plays a protective role in some cells and tissues by internalizing Fe, for example, so that the cells can manage its toxic properties better and/or withhold the Fe from microbial invaders; and (c) does DMT1 transport endanger cells and tissues by internalizing Ni or Pb, for example, placing the toxic metals closer to where they damage cellular functions?

REFERENCES

1   Ponka, P. (2003) Recent advances in cellular iron metabolism. J. Trace Elem. Exp. Med. **16**, 201–217

2   Roth, J. A. and Garrick, M. D. (2003) Iron interactions and other biological reactions mediating the physiological and toxic actions of manganese. Biochem. Pharmacol. **66**, 1–13

3   Gunshin, H., Mackenzie, B., Berger, U. V., Gunshin, Y., Romero, M. F., Boron, W. F., Nussberger, S., Gollan, J. L. and Hediger, M. A. (1997) Cloning and characterization of a mammalian proton-coupled metal-ion transporter. Nature (London) **388**, 482–488

4   Fleming, M. D., Trenor, C. I., Su, M. A., Foernzler, D., Beier, D. R., Dietrich, W. F. and Andrews, N. C. (1997) Microcytic anaemia mice have a mutation in Nramp2, a candidate iron transporter gene. Nature Genet. **16**, 383–386

5   Fleming, M. D., Romano, M. A., Su, M. A., Garrick, L. M., Garrick, M. D. and Andrews, N. C. (1998) Nramp2 is mutated in the anemic Belgrade (b) rat: evidence of a role for Nramp2 in endosomal iron transport. Proc. Natl. Acad. Sci. U.S.A. **95**, 1148–1153

6   Garrick, M. D., Gniecko, K., Liu, Y., Cohan, D. S. and Garrick, L. M. (1993) Transferrin and the transferrin cycle in Belgrade rat reticulocytes. J. Biol. Chem. **268**, 14867–14874

7   Farcich, E. A. and Morgan, E. H. (1992) Uptake of transferrin-bound and nontransferrin-bound iron by reticulocytes from the Belgrade laboratory rat: comparison with Wistar rat transferrin and reticulocytes. Am. J. Hematol. **39**, 9–14

8   Garrick, L. M., Dolan, K. G., Romano, M. A. and Garrick, M. D. (1999) Non-transferrin-bound iron uptake in Belgrade and normal rat erythroid cells. J. Cell. Physiol. **178**, 349–358

9   Garrick, M. D., Singleton, S. T., Vargas, F., Kuo, H., Zhao, L., Knöpfel, M., Davidson, T., Costa, M., Paradkar, P., Roth, J. A. and Garrick, L. M. (2005) DMT1: which metals does it transport? Biol. Res. **39**, 79–85

10   Mackenzie, B. and Garrick, M. D. (2005) Iron imports. II. Iron uptake at the apical membrane in the intestine. Am. J. Physiol. Gastrointest. Liver Physiol. **289**, G981–G986

11   Hubert, N. and Hentze, M. W. (2002) Previously uncharacterized isoforms of divalent metal transporter (DMT)-1: implications for regulation and cellular function. Proc. Natl. Acad. Sci. U.S.A. **99**, 12345–12350

12   Wardrop, S. L. and Richardson, D. R. (1999) The effect of intracellular iron concentration and nitrogen monoxide on Nramp2 expression and non-transferrin-bound iron uptake. Eur. J. Biochem. **263**, 41–49

13   Garrick, M. D. and Garrick, L. M. (2004) Divalent metal transporter DMT1 (SLC11A2). In Membrane Transporter Diseases (Broer, S. and Wagner, C., eds.), pp.107–122, Kluwer, Dordrecht

14   Ghio, A. J., Carter, J. D., Richards, J. H., Crissman, K. M., Bobb, H. H. and Yang, F. M. (2000) Diminished injury in hypotransferrinemic mice after exposure to a metal-rich particle. Am. J. Physiol. Lung Cell. Mol. Physiol. **278**, L1051–L1061

15   Wang, X. C., Ghio, A. J., Yang, F. M., Dolan, K. G., Garrick, M. D. and Piantadosi, C. A. (2002) Iron uptake and Nramp2/DMT1/DCT1 in human bronchial epithelial cells. Am. J. Physiol. Lung Cell. Mol. Physiol. **282**, L987–L995

16   Ghio, A. J., Wang, X. C., Silbajoris, R., Garrick, M. D., Piantadosi, C. A. and Yang, F. M. (2003) DMT1 expression is increased in the lungs of hypotransferrinemic mice. Am. J. Physiol. Lung Cell. Mol. Physiol. **284**, L938–L944

17   Turi, J. L., Yang, F. M., Garrick, M. D., Piantadosi, C. A. and Ghio, A. J. (2004) The iron cycle and oxidative stress in the lung. Free Radic. Biol. Med. **36**, 850–857

18   Ghio, A. J., Wang, X., Dailey, L. A., Stonehuerner, J. D., Piantadosi, C. A., Yang, F., Dolan, K. G., Garrick, L. M. and Garrick, M. D. (2005) Divalent metal transporter-1 decreases metal-related injury in the lung. Am. J. Physiol. Lung Cell. Mol. Physiol. **289**, L460–L467

19   Scheiber-Mojdehkar, B., Sturm, B., Plank, L., Kryzer, I. and Goldenberg, H. (2003) Influence of parenteral iron preparations on non-transferrin bound iron uptake, the iron regulatory protein and the expression of ferritin and the divalent metal transporter DMT-1 in HepG2 human hepatoma cells. Biochem. Pharmacol. **65**, 1973–1978

20   Sturm, B., Goldenberg, H. and Scheiber-Mojdehkar, B. (2003) Transient increase of the labile iron pool in HepG2 cells by intravenous iron preparations. Eur. J. Biochem. **270**, 3731–3738

21   Chen, H., Davidson, T., Singleton, S., Garrick, M. D. and Costa, M. (2005) Nickel decreases cellular iron level and converts cytosolic aconitase to iron regulated protein 1 in A549 cells. Toxicol. Appl. Pharmacol. **206**, 275–287

22   Elisma, F. and Jumarie, C. (2001) Evidence for cadmium uptake through Nramp2: metal speciation studies with Caco-2 cells. Biochem. Biophys. Res. Commun. **285**, 662–668

23   Olivi, L., Sisk, J. and Bressler, J. (2001) Involvement of DMT1 in uptake of Cd in MDCK cells: role of protein kinase C. Am. J. Physiol. Cell Physiol. **281**, C793–C800

24   Tallkvist, J., Bowlus, C. L. and Lönnerdal, B. (2001) DMT1 gene expression and cadmium absorption in human absorptive enterocytes. Toxicol. Lett. **122**, 171–177

25   Bannon, D. I., Portnoy, M. E., Olivi, L., Lees, P., Culotta, V. C. and Bressler, J. P. (2002) Uptake of lead and iron by divalent metal transporter 1 in yeast and mammalian cells. Biochem. Biophys. Res. Commun. **295**, 978–984

26   Kuo, H. C., Smith, J. J., Lis, A., Zhao, L., Gonsiorek, E. A., Zhou, X., Higgins, D. M., Roth, J. A., Garrick, M. D. and Garrick, L. M. (2004) Computer-identified nuclear localization signal in exon 1A of the transporter DMT1 is essentially ineffective in nuclear targeting. J. Neurosci. Res. **76**, 497–511

27   Roth, J. A., Horbinski, C., Feng, L., Dolan, K. G., Higgins, D. and Garrick, M. D. (2000) Differential localization of divalent metal transporter 1 with and without iron response element in rat PC12 and sympathetic neuronal cells. J. Neurosci. **20**, 7595–7601

28   Quail, E. A. and Morgan, E. H. (1994) Role of membrane surface potential and other factors in the uptake of non-transferrin-bound iron by reticulocytes. J. Cell. Physiol. **159**, 238–244

29   Knöpfel, M., Zhao, L. and Garrick, M. D. (2005) Transport of divalent transition-metal ions is lost in small-intestinal tissue of b/b Belgrade rats. Biochem. **44**, 3454–3465

30   Gossen, M. and Bujard, H. (1992) Tight control of gene expression in mammalian cells by tetracycline-responsive promoters. Proc. Natl. Acad. Sci. U.S.A. **89**, 5547–5551

31   Tabuchi, M., Tanaka, N., Nishida-Kitayama, J. O. and Kishi, F. (2002) Alternative splicing regulates the subcellular localization of divalent metal transporter 1 isoforms. Mol. Biol. Cell **13**, 4371–4387

32   Gruenheid, S., Canonne-Hergaux, F., Gauthier, S., Hackam, D. J., Grinstein, S. and Gros, P. (1999) The iron transport protein NRAMP2 is an integral membrane glycoprotein that colocalizes with transferrin in recycling endosomes. J. Exp. Med. **189**, 831–841

33   Lam-Yuk-Sung, S., Touret, N., Grinstein, S. and Gros, P. (2005) Carboxy-terminus determinants of the iron transporter DMT1/SLC11A2 isoform II (− IRE/1B) mediate internalization from the plasma membrane into recycling endosomes. Biochem. **44**, 12149–12159

34   Bowen, B. J. and Morgan, E. H. (1987) Anemia of the Belgrade rat: evidence for defective membrane transport of iron. Blood **70**, 38–44

35   Canonne-Hergaux, F., Gruenheid, S., Ponka, P. and Gros, P. (1999) Cellular and subcellular localization of the Nramp2 iron transporter in the intestinal brush border and regulation by dietary iron. Blood **93**, 4406–4417

36   Canonne-Hergaux, F., Levy, J. E., Fleming, M. D., Montross, L. K., Andrews, N. C. and Gros, P. (2001) Expression of the DMT1 (NRAMP2/DCT1) iron transporter in mice with genetic iron overload disorders. Blood **97**, 1138–1140

37   Yeh, K. Y., Yeh, M., Watkins, J. A., Rodriguez, P. J. and Glass, J. (2000) Dietary iron induces rapid changes in rat intestinal divalent metal transporter expression. Am. J. Physiol. Gastrointest. Liver Physiol. **279**, G1070–G1079

38   Ma, Y. X., Specian, R. D., Yeh, K. Y., Yeh, M., Rodriguez, P. J. and Glass, J. (2002) The transcytosis of divalent metal transporter 1 and apo-transferrin during iron uptake in intestinal epithelium. Am. J. Physiol. Gastrointest. Liver Physiol. **283**, G965–G974

39   Abboud, S. and Haile, D. J. (2000) A novel mammalian iron-regulated protein involved in intracellular iron metabolism. J. Biol. Chem. **275**, 19906–19912

40   McKie, A. T., Marciani, P., Rolfs, A., Brennan, K., Wehr, K., Barrow, D., Miret, S., Bomford, A., Peters, T. J., Farzaneh, F. et al. (2000) A novel duodenal iron-regulated transporter, IREG1, implicated in the basolateral transfer of iron to the circulation. Mol. Cell **5**, 299–309

41   Donovan, A., Brownlie, A., Zhou, Y., Shepard, J., Pratt, S. J., Moynihan, J., Paw, B. H., Drejer, A., Barut, B., Zapata, A. et al. (2000) Positional cloning of zebrafish ferroportin1 identifies a conserved vertebrate iron exporter. Nature (London) **403**, 776–781

42   Nelson, N., Sacher, A. and Nelson, H. (2002) The significance of molecular slips in transport systems. Nat. Rev. Mol. Cell Biol. **3**, 876–881

43   Nevo, Y. and Nelson, N. (2004) The mutation F227I increases the coupling of metal ion transport in DCT1. J. Biol. Chem. **279**, 53056–53061

44   Conrad, M. E., Umbreit, J. N., Moore, E. G., Hainsworth, L. N., Porubcin, M., Simovich, M. J., Nakada, M. T., Dolan, K. and Garrick, M. D. (2000) Separate pathways for cellular uptake of ferric and ferrous iron. Am. J. Physiol. Gastrointest. Liver Physiol. **279**, G767–G774

45   Worthington, M. T., Browne, L., Battle, E. H. and Luo, R. Q. (2000) Functional properties of transfected human DMT1 iron transporter. Am. J. Physiol. Gastrointest. Liver Physiol. **279**, G1265–G1273

46   Mackenzie, B., Ujwal, M. L., Chang, M., Romero, M. F. and Hediger, M. A. (2006) Divalent metal-ion transporter DMT1 mediates both H^+-coupled Fe^{2+} transport and uncoupled fluxes. Pflügers Archiv. Eur. J. Physiol. **451**, 544–548